

Outage Prediction for URLLC in Rician Fading

Andreas Traßl^{1,2}, Tom Hößler³, Lucas Scheuvsen¹, Nick Schwarzenberg¹, and Gerhard P. Fettweis^{1,2,3}

¹Vodafone Chair Mobile Communications Systems, Technische Universität Dresden, Germany

²Centre for Tactile Internet with Human-in-the-Loop (CeTI)

³Barkhausen Institut, Dresden, Germany

Email: {andreas.trassl, lucas.scheuvsen, tom.hoessler, gerhard.fettweis}@tu-dresden.de

Abstract—By scheduling users to resources that are operational rather than on a best effort basis, the overall resource consumption of ultra-reliable low-latency communications (URLLC) can be reduced while maintaining a desired quality of service (QoS). To overcome the time delay between monitoring the channel state and the actual payload transmission, predictive methods which are tailored to the needs of URLLC become indispensable. In this paper we extend our Wiener filter based Rayleigh fading outage predictor to the Rician fading case. Compared to Rayleigh fading, additional estimators for the line of sight (LOS) parameters are presented. Our results show that the overall outage prediction performance increases significantly with increasing power of the LOS component compared to the Rayleigh fading case. The resource utilization for a particular user equipment (UE) rises to more than 99% in the investigated scenario for small prediction horizons and a Rician K -factor of $K = 10$ while achieving effective outage probabilities of 10^{-5} . By comparing with the case of perfect parameter estimation, we show that the influence of the introduced estimators on the outage prediction performance is within acceptable limits.

Index Terms—channel prediction, URLLC, radio resource scheduling

I. INTRODUCTION

Ultra-reliable low-latency communications (URLLC) is foreseen to enable a wide variety of novel applications. In industrial scenarios, current developments aim towards increased production flexibility, more individualization and shorter product cycles [1]. Wireless URLLC is envisioned to support these goals by replacing cables even in many closed-loop control systems. Another application of URLLC is in the field of the Tactile Internet, which is expected to revolutionize health care, education and robotics amongst others [2]. The intuitiveness of certain applications with humans involved heavily relies on round trip latency values of some milliseconds, e.g., in teleoperation systems and virtual environments.

Realizing the ambitious requirements regarding latency and reliability poses a challenge to the communications system. The small-scale fading of the wireless link, which causes random fluctuations of the receive power, is especially demanding. In case of a deep fade, where the instantaneous receive power is very low, packet errors are likely. Concurrently, we consider a wireless link as operational if it provides sufficient signal/noise ratio (SNR) to facilitate an error-free transmission. The commonly used two-state fading model, where the channel is classified in the channel states *up* and *outage* based on a threshold value, is built upon these considerations.

To reduce the probability of deep fades, multi-connectivity can be employed. By transmitting redundant data on multiple links in parallel, a deep fade on a single link is less critical as long as other links stay operational. However, the overall resource consumption of the transmission grows significantly. For example, in order to realize effective outage probabilities of 10^{-5} at a fading margin of 10 dB, at least five independent Rayleigh fading links with selection combining are needed [3]. For lower probabilities, which are in discussion for URLLC, even more links are required. Multi-connectivity is designed to improve reliability at the expense of wasteful resource usage, which raises the question of scalability when many URLLC devices need to be served simultaneously. A solution to this problem is to monitor the channel state and only schedule users to links which are operational. Due to the spatial variation of the fading, resources that lead to transmission errors for one user can be operational for another. Thus, a scheduler with channel knowledge available is expected to reduce the overall resource consumption while maintaining the desired quality of service (QoS) of URLLC. Since monitoring the channel comes at a cost, monitoring signals can be used only occasionally. With the wireless channel also changing over time, the available information quickly becomes outdated and, hence, require the utilization of channel prediction methods.

In literature, various small-scale fading channel predictors have been proposed and analyzed [4], [5]. Recently also machine learning techniques were considered [6], [7]. Analysis in these studies focuses on average prediction errors or spectral efficiency. For URLLC, however, the main optimization goal is the QoS of the individual user. In our previous work [8], we contributed to fill this gap by proposing and analyzing an outage predictor for URLLC, which was designed for the Rayleigh fading case. However, in many scenarios a strong line-of-sight (LOS) component is present. Rician fading was found to be a valid assumption in industrial environments [9], [10], which makes this type of fading important for many URLLC use cases. Therefore, the logical next step is to extend the predictor to the more general Rician fading, which is the topic of this paper. Since Rayleigh fading is a special case of Rician fading, the outage predictor of this paper is also applicable to the Rayleigh fading case. By comparing the performance for Rayleigh fading with our previous work [8], we demonstrate the little influence of the newly introduced predictor components. By means of extensive computer simulations we furthermore

show that the outage prediction performance improves significantly when a LOS component is present. An extension of the results of this paper is available in [11], where also the predictor parameters for the Rician fading case are investigated and application agnostic performance results are presented.

II. SYSTEM MODEL

The channel of interest in this paper is a Rician fast fading channel with its in-phase and quadrature (I/Q) channel coefficient [12]

$$h(t) = \sqrt{2}\sigma \cdot h_{\text{NLOS}}(t) + A \cdot h_{\text{LOS}}(t) \quad . \quad (1)$$

The random non-line-of-sight (NLOS) component $\sqrt{2}\sigma \cdot h_{\text{NLOS}}(t)$ corresponds to Rayleigh fading, which assumes a large number of independently scattered waves arriving at the receive antenna simultaneously. Therefore, the power normalized NLOS component $h_{\text{NLOS}}(t)$ is modeled as zero-mean complex Gaussian variable with unit variance

$$h_{\text{NLOS}}(t) \sim \mathcal{CN}(0, 1) \quad . \quad (2)$$

The scattered waves of the NLOS component are assumed to arrive solely in the horizontal plane with equally distributed angle of arrivals. Furthermore, we assume a constant relative movement between user equipment (UE) and base station (BS) which leads to the classical Doppler spectrum. It is well known that under these assumptions the autocovariance function $r_{\text{NLOS}}(\tau)$ of the NLOS component follows $r_{\text{NLOS}}(\tau) = 2\sigma^2 J_0(2\pi f_m \tau)$. Here J_0 denotes the zeroth order Bessel function of the first kind, which is parameterized by the maximum Doppler spread f_m .

The power normalized LOS component $h_{\text{LOS}}(t)$ is modeled purely deterministic following

$$h_{\text{LOS}}(t) = \exp(j(2\pi f_{D,\text{LOS}}(t - t_0) + \varphi_0)) \quad . \quad (3)$$

Here, $f_{D,\text{LOS}}$ is the Doppler frequency of the LOS component, φ_0 is the initial phase and t_0 is the reference time.

In Rician fading the K -factor is defined as the ratio of power in the LOS component Ω_{LOS} over the power in the NLOS component Ω_{NLOS}

$$K = \frac{\Omega_{\text{LOS}}}{\Omega_{\text{NLOS}}} = \frac{A^2}{2\sigma^2} \quad . \quad (4)$$

Thus, the standard deviation of the complex NLOS component $\sqrt{2}\sigma$ and the amplitude of the LOS component A in (1) can alternatively be expressed over the K -factor and the average channel power $\Omega = \Omega_{\text{LOS}} + \Omega_{\text{NLOS}}$ using

$$\sqrt{2}\sigma = \sqrt{\frac{\Omega}{K+1}}, \quad A = \sqrt{\frac{\Omega K}{K+1}} \quad . \quad (5)$$

A. Channel Estimation

Knowledge over the channel history is assumed to be available through channel estimations. Therefore, a column vector \mathbf{p} consisting of P pilot symbols is transmitted periodically for channel estimation at time t . The received symbols

$$\mathbf{y} = \mathbf{p} \cdot h(t) + \mathbf{n} \quad , \quad (6)$$

are the transmitted pilots \mathbf{p} altered by the channel coefficient $h(t)$ and complex white Gaussian noise (CWGN) \mathbf{n} with variance $2\sigma_n^2$. The minimum variance unbiased (MVU) channel estimator [13] is given by

$$\hat{h}(t) = (\mathbf{p}^H \mathbf{p})^{-1} \mathbf{p}^H \mathbf{y} \quad . \quad (7)$$

Inserting (6) in (7) yields

$$\hat{h}(t) = h(t) + n'(t) \quad . \quad (8)$$

Thus, under the given assumptions the estimate of the channel coefficient $\hat{h}(t)$ is superimposed by CWGN as well, but with variance $2\sigma_{n'}^2 = 2\sigma_n^2 (\mathbf{p}^H \mathbf{p})^{-1}$. The relationship between channel coefficient and noise (8) is an essential part for the derivation of the predictor.

B. Two State Fading Model

The channel is classified in two states *up* and *outage*. The respective channel state is based on the relation of the channel gain to a chosen threshold value $|h_{\text{min}}|$. A different form to characterize the threshold $|h_{\text{min}}|$ is the fading margin $F = |h_{\text{avg}}|^2 / |h_{\text{min}}|^2$, which relates the threshold $|h_{\text{min}}|$ to the average channel gain $|h_{\text{avg}}|$. When the channel gain is greater than the threshold $|h(t)| > |h_{\text{min}}|$ the current channel state is denoted as up. In the up-state the SNR at the receiver is high enough for an URLLC application to be working satisfactorily. Packet errors are still possible in the up-state, but the probability for errors is low enough and long error bursts are seldom. Concurrently, when the channel gain is below the threshold value $|h(t)| < |h_{\text{min}}|$ an outage occurs. In the outage-state the SNR is usually too low for successful decoding, leading to high probabilities of packet errors and long error bursts.

III. RICIAN FADING OUTAGE PREDICTOR

Our objective is to predict outages in a Rician fading channel based on a history of I/Q channel estimations. The predictor we use is a modified version of the Wiener filter based outage predictor for Rayleigh fading, which we have developed in our previous work [8]. The full structure of the outage predictor is shown in Fig. 1 and summarized here.

The channel gain in the Rician fading case has a non-zero mean in the form of the LOS-component, which is important when utilizing a Wiener filter. The strategy when dealing with non-zero mean processes is to subtract the mean before filtering and adding the mean back again to the Wiener filter output [14]. Since we can hardly assume that the LOS component is known, the Rician fading outage predictor has to utilize estimators for the LOS parameters A , $f_{D,\text{LOS}}$ and φ_0 in the first instance. The estimated LOS parameters are then used to calculate the LOS component at time t . After subtraction of the LOS component, the filter coefficients are calculated and the NLOS component is predicted. The LOS parameters are then used to calculate a prediction of the LOS component at time $t + t_p$ which is then added to the Wiener filter output. After summation of the LOS component a predicted I/Q channel sample is available. However, since we are only interested if the channel state will be up or in outage, the predicted I/Q

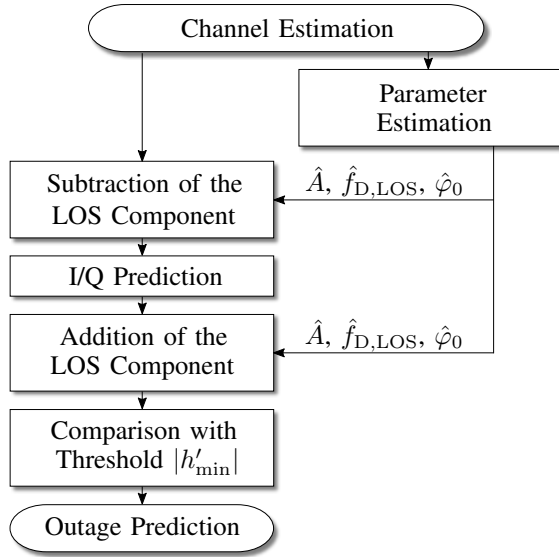


Fig. 1. Structure of the outage predictor for Rician fading.

channel coefficient is eventually compared with a threshold $|h'_{\min}|$. After that, an outage prediction is available which can be used, e.g., for scheduling purposes. All the steps from LOS parameter estimation to the comparison with the threshold are repeated when a new prediction needs to be calculated. In the rest of the section we give a more detailed explanation of the mentioned steps.

A. Parameter Estimation

In a first stage, the parameters of the LOS component A , $f_{D,NLOS}$, φ_0 need to be estimated from a history of channel estimations. For the parameterization of the autocovariance which is needed during calculation of the Wiener filter coefficients, knowledge of the maximum Doppler frequency f_m , the variance of the NLOS component $2\sigma^2$ and the noise variance $2\sigma_n^2$, is needed as well. However, since in measured fading channels the autocovariance is directly estimated anyways, we do not introduce individual estimators for these parameters in this paper. Investigating the performance of the outage predictor in measured fading channel is beyond the scope of this paper. Thus, we assume that these parameters are known and fix from previous observations.

After inserting (1) in (8) an estimation problem is described, where $2\sigma^2$, A , $f_{D,LOS}$ and φ_0 are the unknown parameters and both the CWGN $n'(t)$ and the random NLOS component $\sqrt{2}\sigma \cdot h_{NLOS}(t)$ act as noise. We neglect the temporal correlation of the NLOS component for parameter estimation, due to complexity while the resulting estimators still perform very well in our use-case of outage prediction as we will show in Sec. V. With both the CWGN and the NLOS component being complex Gaussian distributed the sum is also complex Gaussian and can be combined into a single variable.

This yields the standard problem of estimating the parameters of a complex sinusoid in CWGN which can be tackled using

a maximum likelihood (ML) estimation approach as shown in [13]. For the special case of noiseless Rician fading, the desired ML estimators were derived in [15]. In the following we summarize the estimators from [15] and employ an optimization to the frequency estimation. To the best of our knowledge it is the first time that such estimators are employed in a channel predictor.

An ML estimation of the frequency

$$\hat{f}_{D,LOS} = -\arg \max \left(\frac{|\varphi' e^T|^2}{e e^H} \right) \quad (9)$$

is determined by maximizing the periodogram with respect to $f_{D,LOS}$. The observation vector for estimation of the LOS component

$$\varphi' = [\hat{h}(t - (N - 1)\Delta t) \quad \dots \quad \hat{h}(t - \Delta t) \quad \hat{h}(t)] \quad (10)$$

consists of N values and is sampled at a discrete sampling time Δt . Furthermore, a vector of exponential terms

$$e = \left[\exp(-j(2\pi f_{D,LOS}(N - 1)\Delta t)) \quad \dots \quad \exp(-j(2\pi f_{D,LOS}\Delta t)) \quad 1 \right] \quad (11)$$

is part of the estimator. Since the true value of the LOS Doppler frequency $f_{D,LOS}$ could be located between the bins of the periodogram, the frequency estimation can be greatly improved by interpolation as shown in [16]. The authors propose an iterative approach, which we also employ in this paper to refine the frequency estimate (9). As suggested by the authors we used two iterations to enhance the frequency estimate.

The ML estimates for the remaining parameters can then be calculated by inserting the frequency estimate in (11) (we denote this vector as \hat{e} in the following) and using

$$\hat{A} = \left| \frac{\varphi' \hat{e}^H}{\hat{e} \hat{e}^H} \right|, \quad (12)$$

$$\hat{\varphi}_0 = \arg \left\{ \frac{\varphi' \hat{e}^H}{\hat{e} \hat{e}^H} \right\}. \quad (13)$$

B. I/Q Prediction

With estimates of the parameters available, a prediction of the Rician fading can be calculated. Since we use a Wiener filter which relies on the input to be zero mean, a prediction of future I/Q channel samples

$$\hat{h}(t + t_p | t) = (\varphi - \hat{A} \cdot \hat{h}_{LOS})\theta + \hat{A} \cdot \hat{h}_{LOS}(t + t_p) \quad (14)$$

consists of the estimated LOS component at prediction time $\hat{A} \cdot \hat{h}_{LOS}(t + t_p)$ added to the finite impulse response (FIR) filter output $(\varphi - \hat{A} \cdot \hat{h}_{LOS})\theta$, when the observation vector

$$\varphi = [\hat{h}(t) \quad \hat{h}(t - \Delta t) \quad \dots \quad \hat{h}(t - (M - 1)\Delta t)] \quad (15)$$

was adjusted for the respective LOS component vector

$$\hat{A} \cdot \hat{h}_{LOS} = \hat{A} \cdot [\hat{h}_{LOS}(t_0) \quad \hat{h}_{LOS}(t_0 - \Delta t) \quad \dots \quad \hat{h}_{LOS}(t_0 - (M - 1)\Delta t)] \quad (16)$$

at the input of the filter. Note, that for the NLOS prediction we allow the observation vector φ to contain a different number of elements M compared to the observation vector φ' used for parameter estimation. However, we keep the same time between observations Δt as we are able to use the same data as for parameter estimation.

In accordance with the Wiener filter theory, the filter coefficient

$$\theta = \mathbf{R}_{\text{NLOS}}^{-1} \mathbf{r}_{\text{NLOS}} \quad (17)$$

can be calculated using the autocovariance matrix \mathbf{R}_{NLOS} of the filter input and the covariance vector between filter input and NLOS component of the channel coefficient \mathbf{r}_{NLOS} . After subtracting the LOS component, the filter input $\varphi - \mathbf{h}_{\text{LOS}}$ is a Rayleigh fading channel. Therefore, the remaining variables \mathbf{R}_{NLOS} and \mathbf{r}_{NLOS} are obtained by

$$[\mathbf{r}_{\text{NLOS}}]_j = 2\sigma^2 J_0(2\pi f_m(t_p + (j-1)\Delta t)) \quad \text{and} \quad (18)$$

$$[\mathbf{R}_{\text{NLOS}}]_{ij} = \begin{cases} 2\sigma^2 J_0(2\pi f_m|j-i|\Delta t), & i \neq j \\ 2\sigma^2 + 2\sigma_{n'}^2, & i = j \end{cases}, \quad (19)$$

following the assumptions formulated in Sec. II. In these equations, i and j denote the row and column index, respectively.

C. Comparison with Threshold

Since we are interested in the question if an up-state or an outage will occur, the predicted I/Q channel coefficient is finally compared with the threshold $|h'_{\text{min}}|$. It is important to note that the threshold value for prediction $|h'_{\text{min}}|$ was chosen differently from the threshold in the two state fading model $|h_{\text{min}}|$ due to the possibility of prediction errors. By using the threshold $|h'_{\text{min}}|$ for the prediction, we are able to adjust the prediction certainty for indicating an up-state as we have already shown in [8] for the Rayleigh fading case. By doing so, the up-state prediction can be tuned to be more conservative such that falsely predicted up-states are seldom, which makes the predictor usable for URLLC scheduling. In return, falsely predicted outages occur more frequently, which the scheduler has to deal with. A numerical evaluation of this trade-off is presented in Sec. V.

IV. PERFORMANCE METRICS

The predicted I/Q samples do not match the true future value perfectly due to prediction errors. Reasons for prediction errors are differences of the LOS parameter estimations from their true values and deviations of the Wiener filter output from an ideal NLOS prediction. Amongst others, both of these error sources depend strongly on the amount of noise within the observations. The first type of error (false alarm) is when an outage is predicted, but no outage is taking place at the time of interest. In this case an URLLC scheduling algorithm, utilizing the outage predictor, would reject the channel for no reason. The second type of error (missed outage) is the opposite case, when an up-state is predicted but an outage is taking place. This type of error is more critical in an URLLC scenario since no measures can be taken against the looming outage. To study

the performance of the developed outage predictor, we propose to utilize the following metrics, which practically reflect both of these error types in the context of URLLC scheduling.

The first metric is defined in a way to assess the utilizability, i.e., how often the observed link can be utilized for URLLC traffic. Here, we use the average probability to have a link be predicted as up

$$\Pr(\text{predicted up}) = \Pr(P_u) \quad , \quad (20)$$

with P_u as the event for the prediction of an up-state. For example, $\Pr(\text{predicted up}) = 0.8$ indicates that the observed link can be considered for URLLC traffic of a particular UE in 80% of the time.

Our second performance metric covers the risk of fatal failures due to prediction errors. We use the compound probability for an up-state prediction, but the channel being truly in outage

$$P(\text{effective outage}) = P(P_u \cup T_u) \quad . \quad (21)$$

Here, T_u denotes the event that the true future value of the channel coefficient is in outage. For example, $\Pr(\text{effective outage}) = 10^{-3}$ indicates that in 0.1% of the time a prediction will result in an outage. Here, we assume that a (perfect) scheduler can prevent any predicted outage. Thus, this metrics enables statements about the reliability of the system. The name of this metric was changed compared to our previous work [8], however, the definition is the same.

V. NUMERICAL EVALUATION

In this section we demonstrate the performance of the outage predictor for the Rician fading case using the metrics from Sec. IV. The evaluation, which is based on extensive simulations, is conducted for an exemplary URLLC scenario and selected numeric values.

A. Scenario

As in our previous work, we consider an industrial scenario where an automated guided vehicle (AGV) receives wireless control information. The numerical values were kept similar for comparability and are summarized in Table I. The AGV is assumed to move with a constant velocity of 1 m/s. The communications system operates at 3.75 GHz in the middle of the frequency band between 3.7 GHz and 3.8 GHz, which was allocated for industrial use in Germany. Hence, a maximum Doppler frequency $f_m = 12.5$ Hz arises. For numerical evaluation, the Rician K -factor is kept constant over a simulation run in this work. In total three different K -factors are investigated to reflect the case of a strong LOS component ($K = 10$), a medium LOS component ($K = 5$) and no LOS component ($K = 0$). The performance is shown for two different mean channel estimation SNRs of 20 dB and 10 dB. In both cases the fading margin is set to $F = 10$ dB. The LOS parameters $f_{D,LOS}$ and φ_0 are varied randomly. In our simulations $N = 256$ and $M = 25$ channel estimations are used for LOS estimation and the Wiener filter, respectively. Periodic channel estimations are assumed to be available every millisecond.

TABLE I
CHOSEN PARAMETERS FOR NUMERICAL EVALUATION.

Parameter	Value
v	1 m/s
f_c	3.75 GHz
K	0, 5, 10
mean channel estimation SNR	20 dB, 10 dB
F	10 dB
N	256
M	25
Δt	1 ms
simulation runs	2×10^8

B. Results

The results in this paper originate from computer simulations following the Monte-Carlo approach. For each prediction horizon t_p , $2 \cdot 10^8$ different I/Q fading predictions were generated. The outage predictions are calculated for a series of thresholds $|h'_{\min}|$. After comparing the predictions with the true future channel state, the probabilities $\Pr(\text{effective outage})$ and $\Pr(\text{predicted up})$ are empirically determined following the law of large numbers.

In Fig. 2 the outage prediction performance is shown for the chosen scenario and a channel estimation SNR of 10 dB, comparable to a receiver operating characteristic (ROC) curve. However, instead of plotting the true positive rate against the false positive rate, we use the metrics $\Pr(\text{predicted up})$ and $\Pr(\text{effective outage})$ for the reasons discussed in Sec. IV. Each curve spans different operating points, which can be adjusted by varying the threshold value h'_{\min} . The performance of the proposed outage predictor for Rician fading is shown as solid lines. We furthermore show the case of perfect parameter estimation as dashed lines, i.e., $\hat{f}_{D,LOS} = f_{D,LOS}$, $\hat{A} = A$ and $\hat{\varphi}_0 = \varphi_0$. In the case of perfect parameter estimation, the outage prediction performance is solely determined by the Wiener filter. Therefore, the difference between solid and dashed lines reveals the influence of the estimators on the outage prediction performance. In the case of $K = 0$ this also allows for direct comparison with our previous work [8]. Finally, we plotted the baseline performance with randomly guessed future outages as dotted lines. The optimal operation point would be in the top left corner in each of the shown plots. However, due to the existence of prediction errors, as discussed in Sec. IV, the predictor does not always achieve a performance close to this optimum. As expected, the larger the prediction horizon t_p , the worse the outage prediction performance.

When comparing the same prediction horizons for different K -factors, one can observe that the outage predictor performs better at high K -factors. For example, when in the case

of $K = 0$ a prediction horizon $t_p = 11$ ms is utilized and the target probability for an effective outage is set to $\Pr(\text{effective outage}) = 10^{-5}$, the observed link is only predicted as up with a 52% probability. However, for $K = 5$ the same prediction horizon and missed outage probability is achieved while the channel is predicted as up with a much higher probability of 88% and for $K = 10$ even 98% is reached. A reason for that is the decrease of randomness for increasing K -factors. The randomness originates from the NLOS component, whose impact is reduced when a strong LOS component is present. Ultimately, the deterministic LOS component is easier to predict resulting in a better outage prediction performance.

When looking at the overall difference between solid and dashed lines, it can be seen that the solid lines are very close to the dashed lines in the investigated scenario for small prediction times. Furthermore, the difference grows with increasing K . Thus, the introduced estimators have a greater influence on the outage prediction for higher K -factors. However, the estimation error decreases with increasing K -factors since the NLOS component acts as noise in the estimation problem. Instead, the reason for the difference lies in the threshold values $|h'_{\min}|$ which are closer to each other for high values of K . Therefore, already small errors in the I/Q predictions can have a strong influence on the outage prediction performance in this case.

In Fig. 3 the performance for an SNR of 10 dB is shown. When comparing with the previous plots one can see that the overall prediction performance is worse for all K -factors due to the lower SNR. For example, for $K = 0$, a prediction horizon of $t_p = 11$ ms and a targeted effective outage probability of $\Pr(\text{effective outage}) = 10^{-5}$, the probability for a predicted up state is only 19%. To avoid these SNR regions the number of pilot symbols P can be increased.

VI. CONCLUSION

To increase the efficiency of a communications system in resource hungry URLLC scenarios, data can be scheduled to resources with sufficiently good quality, instead of adding redundancy on a best effort basis. To overcome the monitoring delay, predictive methods for fast-fading channels need to be utilized. The proposed Rician fading outage predictor extends our Rayleigh fading outage predictor, by allowing the channel coefficient to contain a LOS component. From our numerical evaluations we can conclude, that the outage prediction performance significantly increases when a LOS component is present compared to the Rayleigh fading case. The higher the proportion of the LOS component, the better the overall outage prediction performance. Our comparison with the case of perfect LOS parameter estimation show, that the influence of the newly introduced estimators on the prediction performance is within acceptable limits. All in all, when measures can be taken in case of an upcoming outage, the predictor has the potential to decrease the effective outage probability on a monitored link many times over. It is left for future work to analyze the performance of the outage predictor under real world conditions.

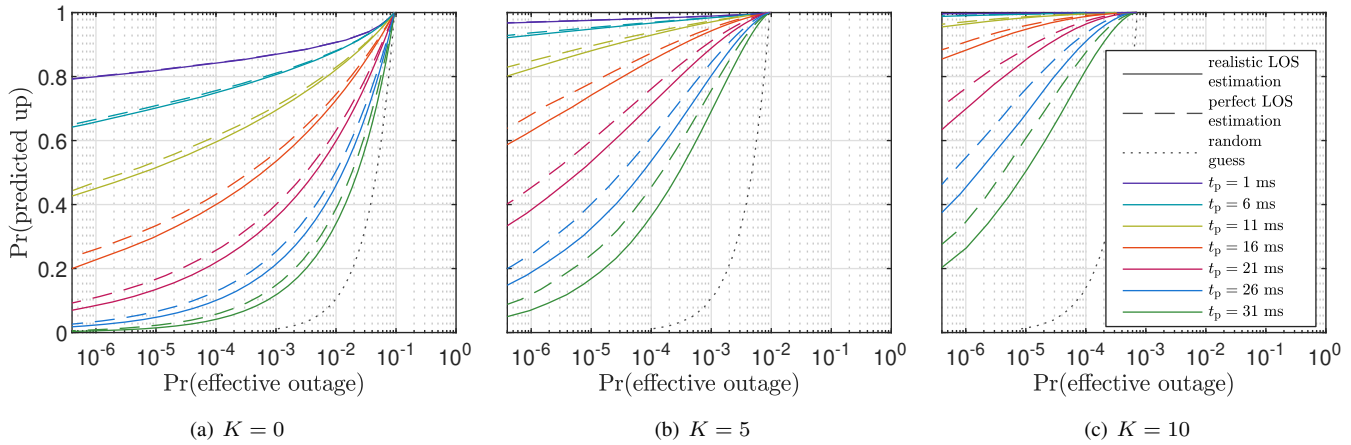


Fig. 2. Predictor performance for the scenario described in Table I, mean channel estimation SNR is 20 dB

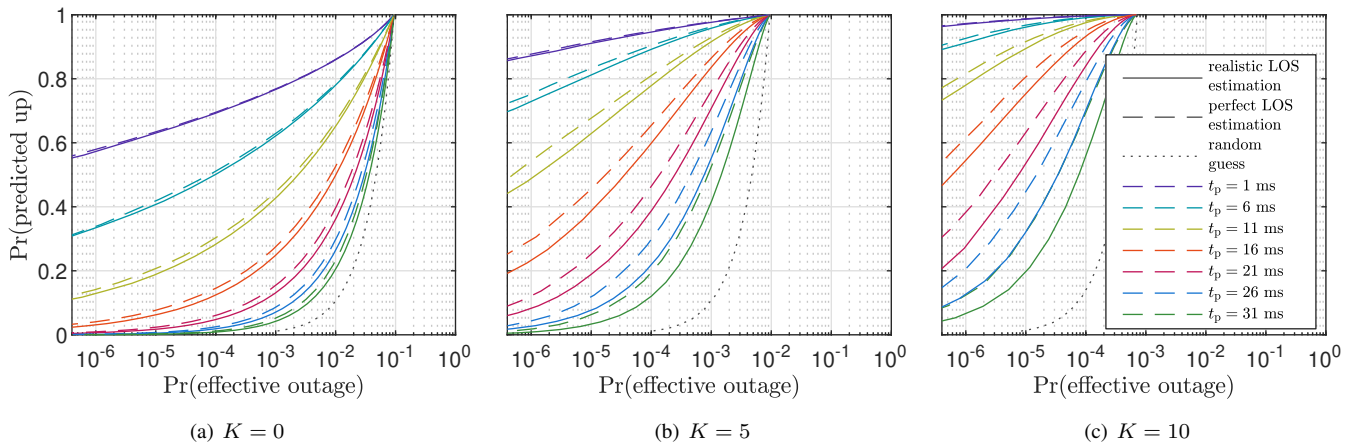


Fig. 3. Predictor performance for the scenario described in Table I, mean channel estimation SNR is 10 dB

ACKNOWLEDGMENTS

This work was in part funded by the German Research Foundation (DFG, Deutsche Forschungsgemeinschaft) as part of Germany's Excellence Strategy – EXC 2050/1 – Project ID 390696704 – Cluster of Excellence “Centre for Tactile Internet with Human-in-the-Loop” (CeTI) of Technische Universität Dresden. This research was co-financed by public funding of the state of Saxony/Germany. We thank the Center for Information Services and High Performance Computing (ZIH) at Technische Universität Dresden for generous allocations of computer time.

REFERENCES

- [1] H. Lasi, P. Fettke, H. Kemper, T. Feld, and M. Hoffmann, “Industry 4.0,” *Bus. & Inform. Syst. Eng.*, vol. 6, no. 4, pp. 239–242, Aug. 2014.
- [2] G. Fettweis, “The tactile internet: applications and challenges,” *IEEE Veh. Technol. Mag.*, vol. 9, no. 1, pp. 64–70, Mar. 2014.
- [3] T. Hößler, M. Simsek, and G. Fettweis, “Joint analysis of channel availability and time-based reliability metrics for wireless URLLC,” in *Proc. 2018 IEEE Global Commun. Conf.*, Dec. 2018.
- [4] T. Ekman, “Prediction of mobile radio channels - modeling and design,” Ph.D. dissertation, Uppsala Univ., 2002.
- [5] A. Duel-Hallen, S. Hu, and H. Hallen, “Long-range prediction of fading signals,” *IEEE Signal Process. Mag.*, vol. 17, no. 3, pp. 62–75, May 2000.
- [6] Y. Zhu, X. Dong, and T. Lu, “An adaptive and parameter-free recurrent neural structure for wireless channel prediction,” *IEEE Trans. Commun.*, vol. 67, no. 11, pp. 8086–8096, Nov. 2019.
- [7] R. Liao, H. Wen, J. Wu, H. Song, F. Pan, and L. Dong, “The Rayleigh fading channel prediction via deep learning,” *Wireless Commun. and Mobile Comput.*, July 2018.
- [8] A. Traßl, L. Scheuven, T. Hößler, E. Schmitt, N. Franchi, and G. Fettweis, “Outage prediction for URLLC in Rayleigh fading,” in *Proc. 29th Eur. Conf. on Networks and Commun.*, June 2020.
- [9] T. Rappaport and C. McGillem, “UHF fading in factories,” *IEEE Journal on Selected Areas in Communications*, vol. 7, no. 1, pp. 40–48, Jan. 1989.
- [10] E. Tanghe, W. Joseph, L. Verloock, L. Martens, H. Capoen, K. Herwegen, and W. Vantomme, “The industrial indoor channel: large-scale and temporal fading at 900, 2400, and 5200 MHz,” *IEEE Transactions on Wireless Communications*, vol. 7, no. 7, pp. 2740–2751, July 2008.
- [11] A. Traßl, E. Schmitt, T. Hößler, L. Scheuven, N. Franchi, N. Schwarzberg, and G. Fettweis, “Outage prediction for ultra-reliable low-latency communications in fast fading channels,” *EURASIP Journal on Wireless Communications and Networking*, vol. 2021, no. 1, pp. 92–117, Apr 2021.
- [12] G. Stüber, *Principles of Mobile Communication*, 4th ed. Springer, 2017.
- [13] S. Kay, *Fundamentals of Statistical Signal Processing: Estimation Theory*. Prentice Hall, 1993.
- [14] A. Oppenheim and G. Verghese, *Signals, Systems and Inference*. Pearson, 2015.
- [15] K. Baddour and T. Willink, “Improved estimation of the Ricean K-factor from I/Q fading channel samples,” *IEEE Transactions on Wireless Communications*, vol. 7, no. 12, pp. 5051–5057, Dec. 2008.
- [16] E. Aboutanios and B. Mulgrew, “Iterative frequency estimation by interpolation on Fourier coefficients,” *IEEE Transactions on Signal Processing*, vol. 53, no. 4, pp. 1237–1242, Mar. 2005.